Latent Heat Flux and Interannual Variability of the Coupled Atmosphere–Ocean System

ZENGXI ZHOU* AND JAMES A. CARTON

Department of Meteorology, University of Maryland at College Park, College Park, Maryland

(Manuscript received 20 July 1995, in final form 9 June 1997)

ABSTRACT

This study examines the impact of the moisture exchange between the oceanic and atmospheric boundary layers on instabilities of the atmosphere–ocean system. Wind speed-sensitive evaporation can affect these instabilities in two ways. First, it can change atmospheric heating and thus modify the atmospheric wind response. Second, it can change the mixed layer heat budget and thus affect SST. Here the authors show that wind speed-sensitive evaporation produces a new unstable, westward-propagating SST mode with a growth rate of (4 month)$^{-1}$ for standard parameters. These two processes, alternatively, act to stabilize the leading unstable mixed SST–dynamics mode if each is considered separately. However, the strongest instability of this mixed SST–dynamics mode occurs when the first process is relatively weak and the second is strong. The authors extend the work to consider the impact of wind speed-sensitive evaporation on the intermediate coupled model of Zebiak and Cane. The results from this model are similar to those obtained in the free mode analysis.

1. Introduction

It is generally accepted that El Niño–Southern Oscillation (ENSO) is the result of instabilities of the coupled atmosphere–ocean system. In the normal mode instability studies of Lau (1981), Hirst (1986), Neelin (1991), and others, the atmosphere influences the ocean through wind stress variations, while the ocean influences the atmosphere by regulating sea surface temperature (SST), which in turn regulates atmospheric convection. These exchange processes are also fundamental to the intermediate coupled model of Zebiak and Cane (1987).

At the same time, satellite-based studies of latent heat flux and solar irradiance by Liu and Gautier (1990) during 1980–83 and ocean buoy measurements by Hayes et al. (1991) both suggest that latent heat fluctuations cannot be neglected, even near the equator. These studies suggest that latent heat loss from the ocean intensifies as the trade winds intensify, thus providing a second process by which surface winds regulate SST. Ocean modeling studies attempting to simulate seasonal and interannual SST have generally been required to include this process (Seager et al. 1988; Giese and Cayan 1993; Koberle and Philander 1994; Carton et al. 1996). Similarly, full coupled atmosphere–ocean general circulation models include both wind stress and latent heating.

Wind speed anomalies impact the moisture exchange between the oceanic and atmospheric boundary layers. The moisture exchange not only affects SST (WESST process, henceforth), but also changes atmospheric heating (WISHE process). Generally, an introduction of a physical process into a system (model) will produce new modes and/or modify existing modes. For example, the WISHE process has been introduced into some simple atmospheric models to explain some features of the 30–60-day oscillations that occur in the Tropics (Neelin et al. 1987; Emanuel 1987; Xie et al. 1993). It is found that this process produces so-called WISHE mode with a timescale of a season or less. While the WISHE process is introduced into a coupled system in this study, it is found that this process functions very differently. In this coupled system, the WISHE process does not produce a new mode, it just modifies the existing coupled low-frequency modes. Mathematically, the coupled modes are directly related to the time derivatives of both atmospheric and oceanic variables (Neelin 1991), while the WISHE mode as identified in previous studies is only related to those of atmospheric variables.

In this study we introduce both the WISHE process and the WESST process in simple and intermediate coupled models. In the following analyses, the two processes will be introduced into the system separately. We find that the WESST process produces an unstable, westward-propagating mode similar to the SST mode of Neelin (1991) but requiring no ocean dynamics. The

* Current affiliation: CIMAS/RSMAS, University of Miami, Miami, Florida.

Corresponding author address: Dr. Zengxi Zhou, NOAA/AOML/PHOD, 4301 Rickenbacker Causeway, Miami, FL 33156.
E-mail: zhou@aoml.noaa.gov

TABLE 1. Basic parameters and their values used in this study. Most of the parameter values in the simple coupled model follow Hirst (1986).

Symbol	Standard value	Parameter
A	5.0×10^{-6} s^{-1}	Atmospheric momentum friction coefficient
B	5.0×10^{-6} s^{-1}	Atmospheric Newtonian cooling coefficient
C_a	30 m s^{-1}	Atmospheric gravity wave speed
C_0	1.4 m s^{-1}	Oceanic gravity wave speed
β	2.2×10^{-11} m^{-1} s^{-1}	Meridional gradient of Coriolis parameter
K_Q	7.0×10^{-3} m^2 s^{-3} K^{-1}	Coefficient controlling SST-related heating
a	1.16×10^{-7} s^{-1}	Oceanic momentum friction coefficient
b	1.16×10^{-7} s^{-1}	Oceanic Newtonian cooling coefficient
d	1.16×10^{-7} s^{-1}	Thermocline damping coefficient
K_T	3.5×10^{-9} K m^{-1} s^{-1}	Coefficient relating thermocline depth to SST
K_s	8.0×10^{-8} s^{-1}	Coefficient relating wind to wind stress
T_x	-5.0×10^{-7} K m^{-1}	Climatological zonal SST gradient
ΔT	14.0 K	Vertical sea temperature difference
h	70.0 m	Mean thermocline depth
h_m	50.0 m	Mean mixed layer depth
α	2.0×10^{-4} K^{-1}	Thermal expansion coefficient of water
g	9.8 m s^{-2}	Gravitational acceleration
C_w	4.2×10^3 K J^{-1} kg^{-1}	Heat capacity of water
ρ_w	1.0×10^3 kg m^{-3}	Water density
F_a	3.5×10^{-3} m s^{-2}	Strength of wind–heating effect
F_a^{cz}	0.4 m s^{-2}	Strength of wind–heating effect in CZ model
F_0	7.3×10^{-8} K m^{-1}	Strength of wind–SST effect
F_0^{cz}	0.5 K s m^{-1}	Strength of wind–SST effect in CZ model
$\lvert\overline{\mathbf{U}}\rvert$	5.5 m s^{-1}	Mean tropical low-level wind speed
$\overline{T}$	298 K	Mean sea surface temperature
L	2.4×10^6 J kg^{-1}	Latent heat constant
δ	0.7	Ratio ($e_{air}/e_s(T)$)
C	9.33×10^{-9} kg Pa m^{-3}	Evaporation constant

WISHE process and the WESST process act to stabilize the unstable mixed SST–oceanic dynamics modes of Philander et al. (1984) and Hirst (1986, 1988), if each process is considered separately. However, the most unstable mode occurs when the WESST process is strong and the WISHE process is relatively weak. When the two processes are introduced into an intermediate coupled model with meridional boundaries, their influences on the ENSO-type oscillation are quite similar to what is found in the free mode analysis. The similarity can be explained by the importance of the free mode instability in the initial development of ENSO events in the intermediate coupled model.

2. Simple model

We begin with the simple coupled anomaly model of Hirst (1986). Surface wind anomalies (U', V') in the baroclinic atmosphere are driven by anomalous atmospheric heating, which is assumed to be controlled by anomalous SST (T') and the WISHE process (F_aU'):

$$AU' - \beta yV' + \phi'_x = 0 \tag{1a}$$

$$AV' + \beta yU' + \phi'_y = 0 \tag{1b}$$

$$C_a^2(U'_x + V'_y) + B'_\phi = -K_QT' + F_aU'. \tag{1c}$$

The ocean consists of an active mixed layer overlying a deep quiescent layer. Horizontal velocity anomalies (u', v') in the mixed layer are induced by surface wind stress fluctuations. The anomalous temperature of the mixed layer, which is assumed to be the same as anomalous sea surface temperature, depends on zonal advection ($\overline{T}_xu'$), mixed layer deepening (K_Th'), Newtonian damping (dT'), and the WESST process (F_0U'). Here the overbar indicates climatological averaging:

$$u'_t - \beta yv' + \alpha g\Delta\overline{T}h'_x + au' = K_sU' \tag{2a}$$

$$v'_t + \beta yu' + \alpha g\Delta\overline{T}h'_y + av' = K_sV' \tag{2b}$$

$$h'_t + \overline{h}(u'_x + v'_y) + bh' = 0 \tag{2c}$$

$$T'_t + \overline{T}_xu' - K_Th' + dT' - F_0U' = 0. \tag{2d}$$

Equations (1) and (2) differ from those of Hirst (1986) only by the addition of wind speed-sensitive latent heating in (1c) and (2d). Equation (2d) was also used by Hirst and Lau (1990), but the influence of the WESST process on the coupled low-frequency instabilities was not discussed by them. Values of constants and definitions are listed in Table 1 and most of them are discussed in Hirst (1986). For simplicity we assume that wind speed-sensitive evaporation depends only on the zonal component of the wind. The sign of the anomalous latent heating term is determined by the direction of the mean trade winds. In the easterly trade wind region, positive zonal wind anomalies imply less wind speed-sensitive evaporation and thus a positive SST change and increasing atmospheric heating. Latent heat flux anomalies (LH') are related to mean total wind speed

$|\overline{\mathbf{U}}|$, saturation vapor pressure at sea surface temperature $e_s(T)$, and ambient vapor pressure, e_a. Following Seager et al. (1988), this relationship may be approximated as

$$\frac{LH'}{C_w\rho_w\overline{h}} = \frac{-LC(1-\delta)|\overline{\mathbf{U}}|}{C_w\rho_w\overline{h}}\left[\frac{\partial e_s}{\partial T}\right]_{T=\overline{T}}T' + \frac{LC(1-\delta)e_s(\overline{T})}{C_w\rho_w\overline{h}}U' \tag{3a}$$

$$\approx (-3.5\times10^{-8}\ \mathrm{s}^{-1})T' + (7.3\times10^{-8}\ \mathrm{K\ m}^{-1})U', \tag{3b}$$

where it is assumed that $\delta = e_a/e_s$ is a constant. The first term on the right-hand side is incorporated in the damping process (dT') in (2d), while the second term is accounted for by the addition of F_0U' in (2d). Thus, we assume $F_0 = 7.3\times10^{-8}$ K m^{-1}. The standard value for the WISHE process, F_a, is taken to be 3.5×10^{-3} m s^{-2}, which makes the ratio K_Q/F_a the same as the value used in Hirst and Lau (1990).

The coupled system [(1) and (2)] contains three kinds of normal mode solutions. They are atmospheric dynamics modes, oceanic dynamics modes, and SST modes, the latter being related to the time derivative of SST in (2d). These three kinds of modes are not well separated and are best described collectively as mixed SST–dynamics modes. But if the ocean dynamics is separated from the rest, and the atmosphere is in equilibrium with SST, then the atmospheric dynamics modes disappear and SST modes and oceanic dynamics modes do separate (Neelin and Jin 1993). We discuss this case first.

The resulting system of equations may be simplified to two equations, one expressing the zonal wind anomalies resulting from SST anomalies, and the other describing how SST responds to the WESST process ($T'_t = F_0U'$). Assuming solutions of the form of $(U', T') = (U_0e^{i\phi}, 1)\tilde{T}(y)\exp(ikx - \sigma t)$, the inclusion of the WESST process into this simplified system produces an unstable westward-propagating SST mode with the growth rate of 1/4 month^{-1} for the standard value of F_0. Here $\phi = 60°$ represents the relative zonal phase of zonal wind anomalies and SST anomalies, and U_0 is 2.5 m s^{-1}. This mode acts in many ways similar to the β-effect Ekman pumping term in the SST mode of Neelin [1991, term A1 in Eq. (53)]. It is distinguished, however, from the SST modes of Neelin (1991) and Jin and Neelin (1993) in that it needs no ocean dynamics. We note that a coupled mode similar to the SST mode identified here was found to be responsible for the westward propagation of annual disturbances in the eastern tropical Pacific region (Liu and Xie 1994).

In addition to producing a new unstable SST mode, inclusion of wind speed-sensitive evaporation modifies the mixed SST–oceanic dynamics modes. We begin our discussion by considering a fixed zonal wavelength of 16 000 km, approximately the width of the Pacific Ocean. Equations (1) and (2) are solved numerically using techniques similar to those of Hirst (1986), assuming a Fourier expansion in zonal direction. The system supports both gravity modes and low-frequency modes. Following Hirst, we will restrict our attention to the low-frequency modes with simple meridional structures.

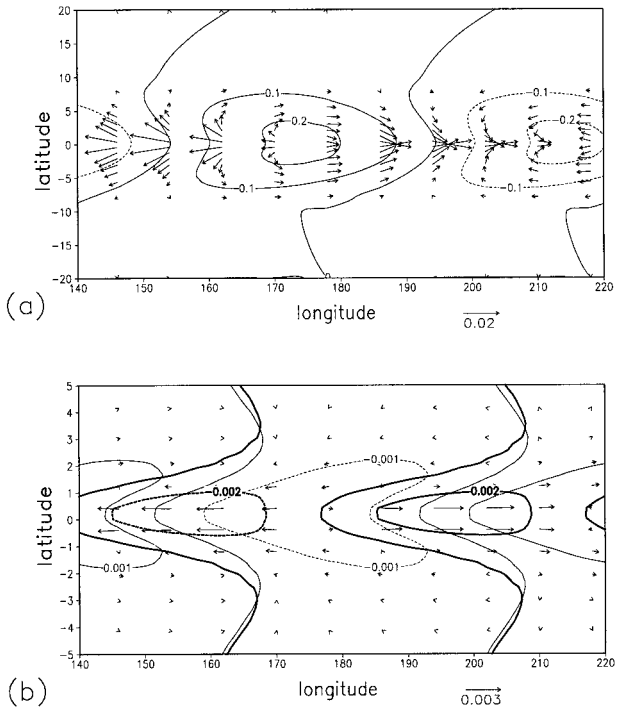

FIG. 1. Spatial pattern of the leading unstable mode in the general case without wind speed-sensitive evaporation. (a) Nondimensional atmospheric wind anomaly (arrow) and pressure anomaly (contour line). Contour interval is 0.1. (b) Nondimensional oceanic current anomaly (arrow), SST anomaly (thick line), and thermocline depth anomaly (thin line). Contour interval is 0.02 for SST and 0.01 for thermocline depth anomaly.

First we consider the full equation (2d). If F_a and F_0 were set to zero, an unstable mode is present that propagates slowly eastward with a phase speed of 0.09 m s^{-1}. The growth rate and period are 1/56 day^{-1} and 1870 days. The spatial structure of this unstable mode is depicted in Fig. 1. Consistent with the Gill-type atmospheric model (Gill 1980), anomalous atmospheric winds converge to the region of anomalous low air pressure. Maximum westerly wind anomalies occur to the west of maximum SST anomalies (Fig. 1a). The meridional scale of atmospheric disturbances is much larger than oceanic disturbances because of their larger deformation radius.

In the ocean (Fig. 1b), the spatial pattern of this mode is similar to that of an uncoupled oceanic Kelvin wave. Meridional currents are negligible, while zonal currents and thermocline depth anomalies are all centered on the equator. Note, however, that zonal currents are shifted westward by $\pi/3$ relative to thermocline depth. Maxi-

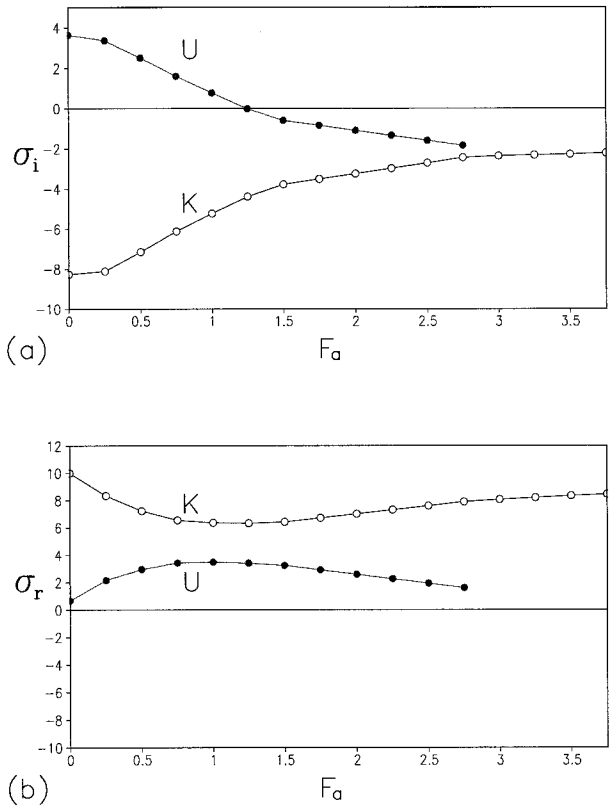

FIG. 2. (a) Growth rate σ_i and (b) frequency σ_r as a function of the strength of the WISHE process, F_a, for the Kelvin wave (open circles) and the leading unstable mode (solid circles) at a wavelength of 16 000 km. Frequency is expressed in units of 1/20800 day^{-1}, growth rate has units of 1/208 day^{-1}, and F_a has units of 10^{-3} m s^{-2}.

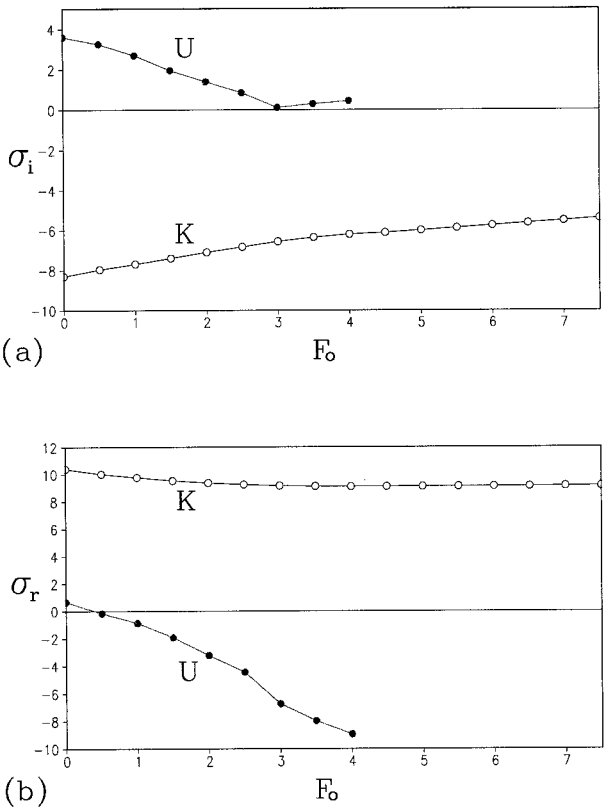

FIG. 3. (a) Growth rate σ_i and (b) frequency σ_r as a function of the strength of the WESST process, F_0, for the Kelvin wave (open circles) and the leading unstable mode (solid circles) at a wavelength of 16 000 km. Frequency is expressed in units of 1/20800 day^{-1}, growth rate has units of 1/208 day^{-1}, and F_0 has units of 10^{-8} K m^{-1}.

mum positive SST anomalies are also shifted to the west of maximum thermocline depth anomalies by $\pi/3$. The explanation for the phase shift lies in the temperature equation, (2d). An eastward-propagating disturbance in the thermocline will produce a maximum SST response to the west by a phase shift of $\pi/2$ if (2d) is dominated by a balance $T_t' - K_T h' = 0$. The phase shift is less than $\pi/2$ if damping is included. The phase relationship between SST, u, and h in this mode suggests that $K_T h'$ is a dominant term in (2d).

a. WISHE process

When K_s is at its standard value, but F_0 is set to zero, increasing F_a acts to stabilize the unstable mode. The unstable mode becomes completely stable for values of $F_a > 1.2 \times 10^{-3}$ m s^{-2} (Fig. 2a). To understand this result, we compare the structure of the original unstable mode to that of the unstable mode when F_a is equal to 7.0×10^{-4} m s^{-2}. When $F_a = 0$, a 1°C SST anomaly corresponds to a maximum westerly wind anomaly of 0.51 m s^{-1} west of the SST anomaly. As F_a increases to 7.0×10^{-4} m s^{-2}, a 1°C SST anomaly produces a 0.48 m s^{-1} maximum westerly anomaly, with SST and wind anomalies almost in phase. The decrease in both the wind response and the phase shift between temperature anomalies and wind anomalies acts to reduce the growth rate of the unstable mode.

b. WESST process

When F_a is set to zero, increasing F_0 also acts to stabilize the unstable mode for $F_0 < 3.0 \times 10^{-8}$ K m^{-1} (Fig. 3a). Moreover, increasing F_0 reduces the eastward speed of the unstable mode. For $F_0 > 3.2 \times 10^{-9}$ K m^{-1} the mode reverses its direction of propagation (Fig. 3b). For this unstable mode, SST change is mainly controlled by a localized balance in the temperature equation in which SST changes reflect changes in thermocline depth. It is also evident that zonal wind anomaly is negatively correlated with the thermocline depth anomaly over equatorial areas if F_0 is small (Fig. 4a). Therefore, in the region where the localized relationship between SST and thermocline depth dominates the temperature equation, increasing latent heat loss reduces this growth. For $F_0 > 3.0 \times 10^{-8}$ K m^{-1}, zonal wind and thermocline depth anomalies become positively correlated (Fig. 4b). Now reduced latent heat loss occurs

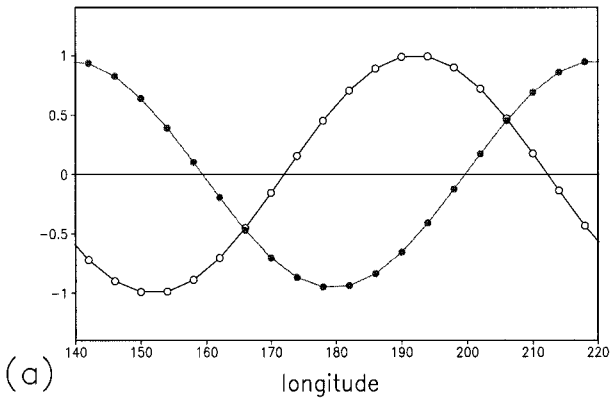

FIG. 4. Normalized nondimensional equatorial atmospheric zonal wind anomaly (open circle) and thermocline depth anomaly (solid circle) in the general case for (a) $F_a = 0$, $F_0 = 0$, and (b) $F_a = 0$, $F_0 = 3.9 \times 10^{-8}$ K m^{-1}.

where SST growth is maximum. Increasing F_0 in this parameter range acts to make the unstable mode more unstable.

c. Combined processes

The discussion above shows that when the WISHE process and the WESST process are considered separately, each acts to stabilize the leading unstable mode. Here we find that when both processes are taken into account, their combined influence is quite different. A contour map of growth rate as a function of F_a and F_0 is presented in Fig. 5. It is evident that the unstable mode becomes most unstable when F_0 takes on large values and F_a is about one-tenth of the suggested value. Unfortunately, the map of growth rate cannot easily be extended to the larger parameter values because of the difficulty of tracing a single mode in this parameter range.

We now consider two limiting cases of the mixed-layer temperature equation. In the first case the mean zonal gradient of SST is set to zero and (2d) reduces to

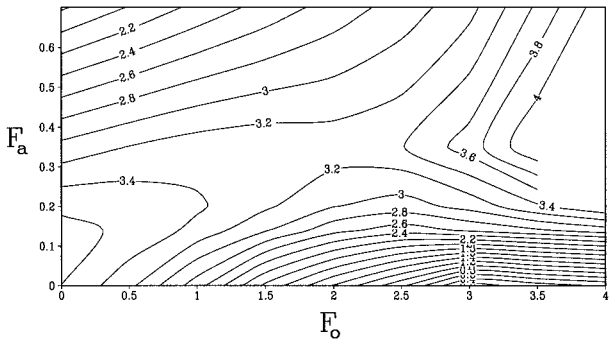

FIG. 5. Nondimensional growth rate of the leading unstable mode in the general case as a function of F_a and F_0. Contour level is 0.2, F_0 has units of 10^{-8} K m^{-1}, and F_a has units of 10^{-3} m s^{-1}.

$$T'_t - K_T h' + dT' - F_0 U' = 0. \tag{4}$$

If F_a and F_0 were set to zero, Hirst (1986) has shown that this system supports an eastward-propagating growing mode with a growth rate of 1/160 day^{-1}, a period of 450 days, and a phase speed of 0.39 m s^{-1}. The inclusion of wind speed-sensitive evaporation has a qualitatively similar effect as in the general case.

In the second case, thermal advection is retained, but the thermocline depth dependence is neglected:

$$T'_t + \overline{T}_x u' + dT' - F_0 U' = 0. \tag{5}$$

In the absence of wind speed-sensitive evaporation there exists a growing mode with a growth rate of 1/77 day^{-1}, a period of 700 days, and a westward phase speed of 0.25 m s^{-1}. Maximum thermocline depth disturbances occur off the equator for this coupled mode, a feature shared by the uncoupled first symmetric Rossby mode. However, this coupled mode is different from an uncoupled oceanic Rossby mode since here zonal velocity and thermocline depth anomalies are out of phase by $\pi/2$ and meridional velocity is negligible.

Here, F_a acts to stabilize the unstable mode because it reduces the coupling strength of the system as discussed in the general case. On the other hand, increasing F_0 acts to make the unstable mode more energetic. In this case the wind anomaly is positively correlated with oceanic velocity anomaly. In the region where there is a maximum SST increase due to thermal advection, the SST increase is enhanced by reduced evaporation. The strongest instabilities occur when F_a is 0 and F_0 is large.

Throughout the discussion above we assumed a fixed wavenumber. In fact, the impact of wind speed-sensitive evaporation is largest for long wavelengths when the full SST equation (2d) is considered. Wind speed-sensitive evaporation has little effect on growth rate for wavelengths less than 5000 km.

3. Intermediate model

The model discussed above is limited by the absence of meridional boundaries and seasonal currents. In order

TABLE 2. Change of ENSO-type oscillations with WISHE process (F_a^{cz}) and WESST process (F_0^{cz}) in the intermediate coupled model. The behavior of the change is divided into three regimes. In regime one, ENSO-type oscillations still exist. In regime three, they disappear. Regime two is a transition zone between regime one and regime three. See corresponding text for discussions.

	F_a^{cz}						
F_0^{cz}	0.0	0.1	0.2	0.3	0.4	0.5	0.6
0.0	1	2	3	3	3	3	3
0.1	3	1	2	3	3	3	3
0.2	3	1	2	2	2	3	3
0.3	3	3	2	3	3	3	3
0.4	3	2	1	2	3	3	3
0.5	3	3	2	1	3	1	3
0.6	3	3	2	1	2	3	3
0.7	3	2	1	1	3	3	3

to include these, we turn to the intermediate coupled atmosphere–ocean model (CZ model) of Zebiak and Cane (1987). This widely used model solves a set of equations similar to (1) and (2) but includes boundaries and the climatological seasonal cycle. There are two reasons why we chose the CZ model. First, the CZ model is able to simulate important aspects of low-frequency variabilities in the tropical Pacific reallistically. Also, it is computationally efficient. One major inadequacy of the CZ model is that its atmospheric component produces unrealistic easterly surface wind anomalies in the eastern Pacific during a warm event.

In the following numerical experiments, the initial conditions are produced by a 50-yr integration of the standard model starting from a condition of rest. The model is then integrated for 70 more years with and without the wind speed-sensitive evaporation. It should be noted that we have repeated some coupled model experiments with different initial conditions, including warm and cold events. It is found that the oscillation patterns in the model are mainly decided by the model parameters, not by the initial conditions.

To introduce the wind speed-sensitive evaporation in the CZ model, part of the atmospheric heating term CT' is replaced with $(CT' + F_a^{cz}|\overline{\mathbf{U}}|')$. Similarly, in the ocean SST equation, dT' is replaced with $(dT' + dF_0^{cz}|\overline{\mathbf{U}}|')$. We choose standard values of F_a^{cz} and F_0^{cz} to ensure that F_a^{cz}/C and dF_0^{cz}/d are the same as the corresponding values in the free mode analysis.

We begin with parameters suggested by Zebiak and Cane for the Pacific Ocean. In the absence of wind speed-sensitive evaporation, area-averaged anomalous SST at NINO3 (5°N–5°S, 90°–150°W) has fluctuations with amplitudes of 1.5°C and periods of 3–4 yr. For a more detailed description of this ENSO-type oscillation in the model the reader is referred to Zebiak and Cane (1987) and Battisti (1988).

The behavior of model oscillations for different F_a^{cz} and F_0^{cz} can be divided into three regimes (Table 2), based on about 70 yr of model integration. In the first regime, the ENSO-type oscillation still exists. Within this regime, the amplitude of oscillation increases with increasing F_0^{cz} and the oscillation period becomes shorter. For $F_a^{cz} = 0.3$ m s^{-2}, $F_0^{cz} = 0.6$ K s m^{-1}, the oscillation period is about 3 yr (Fig. 6a). Comparison of the amplitudes of oscillations indicates that the most energetic oscillation occurs when the WISHE process is relatively weak (around $F_a^{cz} = 0.3$ m s^{-2}) and the WESST process is strong. It should be noted that this regime covers a narrow parameter space, as shown in Table 2.

In the third regime, which covers a large parameter space in Table 2, ENSO-type oscillations have disappeared by the end of the integration (Fig. 6c). Situated between the first and third regime is regime two. In this regime, the ENSO-type oscillations are not as clearly identified as in regime one, or the oscillations exist for some time, then disappear, and then come back again within the 70-yr integration. For example, at $F_a^{cz} = 0.2$ m s^{-2}, and $F_0^{cz} = 0.2$ K s m^{-1}, the ENSO-type oscillations exist for about 15 yr. For the next 10 yr, they weaken. Starting at model year 30, the coupled model evolved into an annual cycle state with nonzero mean. Finally, around model year 50, the ENSO-type oscillations come back again (Fig. 6b). As in the case of the simple coupled system, either the WISHE process or the WESST process alone stabilizes the leading unstable modes.

4. Conclusions

The effects of latent heating have been largely ignored in recent studies of the instabilities of the coupled atmosphere–ocean system. This is surprising since observational studies from the eastern Pacific suggest that latent heating is a dominant term in the anomalous heat budget of the oceanic mixed layer. In this study we examine the effects of latent heating on coupled instabilities in two classes of models: simple analytic models and an intermediate numerical models.

It is found that the WESST process produces a new SST mode. The effect of anomalous latent heating on the heat budget of the oceanic mixed layer may be parameterized as two terms, one proportional to anomalous SST, and the other proportional to anomalous surface wind speed. The first term is positive when SST is anomalously low, and negative when SST is anomalously high, and so acts to dampen anomalous SST. Whether the second term makes a positive or negative contribution mainly depends on the importance of ocean dynamics. If ocean dynamics is unimportant, then a westward-propagating instability will develop in which a patch of anomalously warm SST is bounded to the west by anomalously weak trade winds and to the east by anomalously strong trade winds. This configuration of winds acts to reinforce the original perturbation through wind speed-sensitive latent heating, while causing it to propagate westward. For the parameters chosen in this study the growth rate is 1/4 month^{-1}. In 1991 Neelin identified a similar mechanism in which surface winds

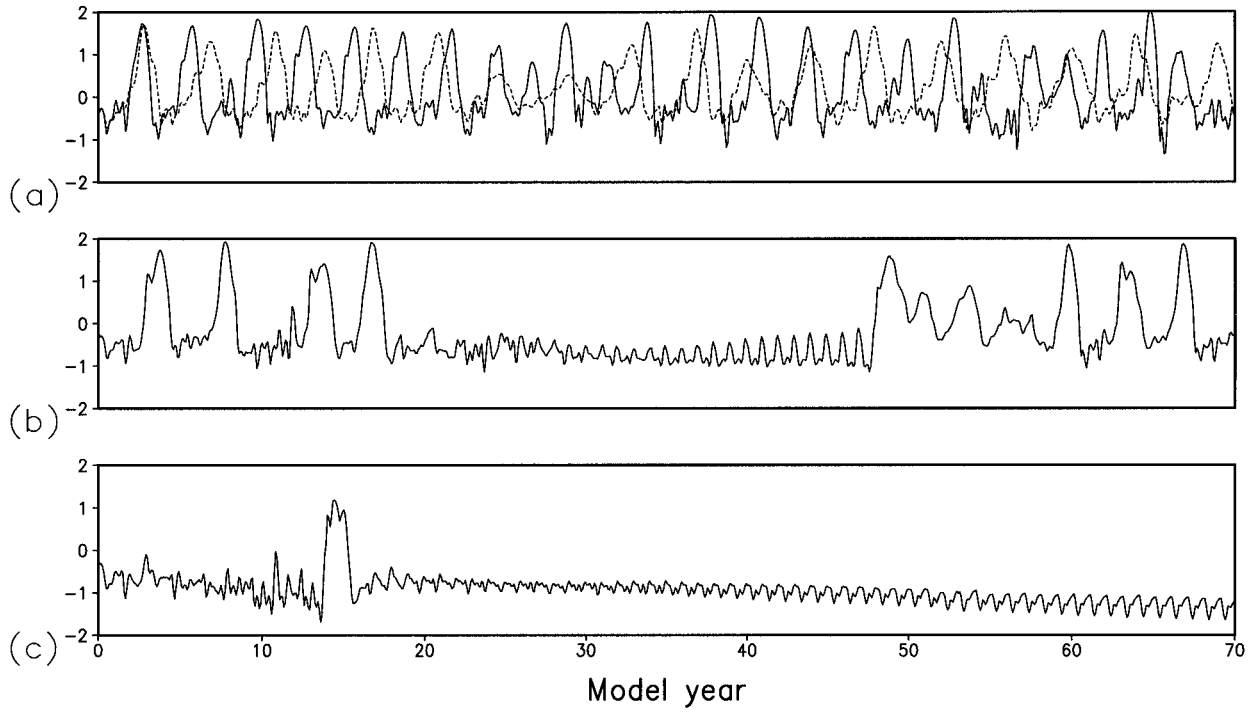

FIG. 6. NINO3 area-averaged SST anomaly (5°N–5°S, 90°–150°W) with time. (a) Regime 1: $F_a^{cz} = 0$, $F_0^{cz} = 0$ (dashed line); $F_a^{cz} = 0.3$ m s^{-2}, $F_0^{cz} = 0.6$ K s m^{-1} (solid line); (b) regime 2: $F_a^{cz} = 0.2$ m s^{-2}, $F_0^{cz} = 0.2$ K s m^{-1}; and (c) regime 3: $F_a^{cz} = 0.4$ m s^{-2}, $F_0^{cz} = 0.1$ K s m^{-1}.

can act in conjunction with Ekman pumping to reinforce an initial perturbation. The mechanism we describe here differs from Neelin's SST mode mainly because no ocean dynamics is required at all. It should be noted that there are many other physical processes that contribute to the growth rate and wave speed of SST modes, making identification of them in observations difficult.

In addition to supporting SST mode instabilities, the tropical atmosphere–ocean system is known to support mixed SST–oceanic dynamics modes of the kind investigated by Philander et al. (1984) and Hirst (1986). Similar instabilities are known to be important in producing interannual variability in the coupled model of Zebiak and Cane (1987). Wind speed-sensitive evaporation can affect these mixed SST–oceanic dynamics modes in two ways. First, it can change the atmospheric heating field and thus affect the strength of the air–sea coupling. For the coupled model of Hirst (1986), we find that the introduction of the WISHE process alone reduces the coupling strength of the system and stabilizes the leading unstable mode. Second, wind speed-sensitive evaporation can modify the mixed layer heat budget and thus change SST. In cases where vertical advection of anomalous temperature plays a dominant role, how the WESST process affects the coupled instability depends on the phase relationship between atmospheric wind speed and thermocline depth anomalies. If a positive wind speed anomaly is overlaying a positive thermocline depth anomaly, the increase in SST due to vertical thermal advection will be reduced due to increasing latent heat loss. Unstable modes in these cases will be stabilized. On the other hand, a negative correlation between wind speed and thermocline depth leads to an amplification of unstable modes.

When wind speed-sensitive evaporation is introduced into an intermediate coupled model with meridional boundaries, its influence on the ENSO-type oscillation is quite similar to what is found in the free mode analysis. The similarity is because of the importance of the free mode instability in the initial development of ENSO events in the intermediate coupled model. Finally, it should be noted that it is interesting to explore the impact of wind speed-sensitive evaporation in a more sophisticated model such as a coupled general circulation model.

Acknowledgments. We sincerely thank Dr. Steve Zebiak for helping to set up the CZ model. This work was supported by the National Science Foundation under Grant OCE9416894. We are grateful to the anonymous reviewers whose valuable comments have contributed greatly to the manuscript.

REFERENCES

Battisti, D. S., 1988: Dynamics and thermodynamics of a warm event in a coupled atmosphere–ocean model. *J. Atmos. Sci.*, **45,** 2889–2919.

Carton, J. A., X. Cao, B. S. Giese, and A. M. da Silva, 1996: Decadal and interannual SST variability in the tropical Atlantic Ocean. *J. Phys. Oceanogr.,* **26,** 1165–1175.

Emanuel, K. A., 1987: An air–sea interaction model of intraseasonal oscillations in the tropics. *J. Atmos. Sci.,* **44,** 2324–2340.

Giese, B. S., and D. R. Cayan, 1993: Surface heat flux parameterizations and tropical Pacific sea surface temperature simulations. *J. Geophys. Res.,* **98,** 6979–6989.

Gill, A., 1980: Some simple solutions for heat induced tropical circulation. *Quart. J. Roy. Meteor. Soc.,* **106,** 447–462.

Hayes, S. P., P. Chang, and M. J. McPhaden, 1991: Variability of the sea surface temperature in the eastern equatorial Pacific Ocean. *J. Geophys. Res.,* **96,** 10 553–10 566.

Hirst, A. C., 1986: Unstable and damped equatorial modes in simple coupled ocean–atmosphere models. *J. Atmos. Sci.,* **43,** 606–630.

——, 1988: Slow instabilities in tropical ocean basin–global atmosphere models. *J. Atmos. Sci.,* **45,** 830–852.

——, and K.-M. Lau, 1990: Intraseasonal and interannual oscillations in coupled ocean–atmosphere models. *J. Climate,* **3,** 713–725.

Jin, F.-F., and J. D. Neelin, 1993: Modes of interannual tropical ocean–atmosphere interaction—A unified view. Part I: Numerical results. *J. Atmos. Sci.,* **50,** 3477–3503.

Koberle, C., and S. G. H. Philander, 1994: On the processes that control seasonal variations of sea surface temperatures in the tropical Pacific Ocean. *Tellus,* **46A,** 481–496.

Lau, K., 1981: Oscillations in a simple equatorial climate system. *J. Atmos. Sci.,* **38,** 248–261.

Liu, W. T., and C. Gauthier, 1990: Thermal forcing on the tropical Pacific from satellite data. *J. Geophys. Res.,* **95,** 13 209–13 217.

Liu, Z., and S. Xie, 1994: Equatorward propagation of coupled air–sea disturbances with application to the annual cycle of the eastern tropical Pacific. *J. Atmos. Sci.,* **51,** 3807–3822.

Neelin, J. D., 1991: The slow sea surface temperature mode and the fast-wave limit: Analytic theory for tropical interannual oscillations and experiments in a hybrid coupled model. *J. Atmos. Sci.,* **48,** 584–606.

——, and F.-F. Jin, 1993: Modes of interannual tropical ocean–atmosphere interaction—A unified view. Part II: Analytical results in the weak-coupling limit. *J. Atmos. Sci.,* **50,** 3504–3522.

——, I. M. Held, and K. H. Cook, 1987: Evaporation-wind feedback and low-frequency variability in the tropical atmosphere. *J. Atmos. Sci.,* **44,** 2341–2348.

Philander, S. G. H., T. Yamagata, and R. C. Pacanowski, 1984: Unstable air–sea interactions in the tropics. *J. Atmos. Sci.,* **41,** 604–613.

Seager, R., S. E. Zebiak, and M. A. Cane, 1988: A model of the tropical Pacific sea surface temperature climatology. *J. Geophys. Res.,* **93,** 1265–1280.

Xie, S. P., A. Kubokawa, and K. Hanawa, 1993: Evaporation-wind feedback and the organizing of tropical convection on the planetary scale. Part I: Quasi-linear instability. *J. Atmos. Sci.,* **50,** 3873–3883.

Zebiak, S., and M. Cane, 1987: A model El Niño–Southern Oscillation. *Mon. Wea. Rev.,* **115,** 2262–2278.